Bandwidth analysis of multimode fiber passive optical networks (PONs)

Grzegorz STEPNIAK*, Lukasz MAKSYMIUK, Jerzy SIUZDAK

Institute of Telecommunications, Warsaw University of Technology, Nowowiejska 15/19,
00-665 Warszawa, Poland

*Corresponding author: stepniak@tele.pw.edu.pl

The analysis of frequency response in different branches of a multimode fiber based passive optical network is conducted. Both the theoretical and experimental results show that bandwidth of various network paths may be different.

1. Introduction

The multimode fiber (MMF), due to its larger core size, has a number of advantages over single mode fiber (SMF) in access and local networks, where the cost and time of installation play substantial role. For the same reason passive optical network (PON) is expected to become the most popular technology in MMF networks.

A lot of work has been devoted to the investigation of MMF parameters, especially its bandwidth, with regard to the possible application of existing MMF LANs for higher bit rates (Gbit/s and 10 Gbit/s Ethernet) [1, 2]. Nevertheless, to the best of authors' knowledge there are hardly any papers treating of the bandwidth performance of PONs incorporating MMFs. This matter is of utmost importance, as modal filtering in the network branching components may affect the node-to-node transmission parameters. In such a situation, to serve the users with equal quality, performance of the whole network has to be adjusted to the lowest available level.

In this paper, we extend the MMF link model [1] by adding a coupler/splitter module and thus we make it possible to analyze frequency response of any optical path within a MMF PON. The effect of splitter influence on the bandwidth is investigated both numerically and experimentally.

2. Theory

We employ the frequency domain analysis and matrix formalism to model the network components, which was first applied in [1]. Let us represent the mode power distribution with a vector [1]:

$$\mathbf{A} = \left[A_1(\omega)...A_M(\omega) \right]^T \tag{1}$$

where M is the highest mode group number in the fiber and T denotes transposition. The elements of $\mathbf{A}$ are complex numbers – their modulus represents power in a mode group, whereas their argument – the group delay of a mode group for angular frequency ω [1].

In our model, the network components – fibers, couplers/splitters and connectors are represented by matrices operating on vectors (1). The modulus of the element $b_{i,j}$ of component matrix $\mathbf{B}$ represents part of the power of the j-th mode group that is transferred to the i-th mode group at this component whereas its argument represents possible delay (only for distributed elements such as fibers). To find the mode power vector at a certain node, the product of matrices on the path from the light source to that node must be computed. For instance, to find the frequency response of the optical path that contains (counting from the light source): a fiber, a connector and a splitter, with receiver in the (a) arm of the splitter, the mode power distribution vector at receiver has to be first computed

$$\mathbf{A}^{(R)}(\omega) = \tilde{\mathbf{S}}^{(a)} \cdot \tilde{\mathbf{C}} \cdot \tilde{\mathbf{F}}(\omega) \cdot \mathbf{A}^{(\text{inp})}(\omega) \tag{2}$$

where $\mathbf{A}^{(\text{inp})}(\omega)$ is the input mode power distribution vector that depends on the launching conditions. We denote the splitter, connector, and fiber matrices with $\tilde{\mathbf{S}}$, $\tilde{\mathbf{C}}$, and $\tilde{\mathbf{F}}$, respectively. The splitter has a different matrix for each arm. Finally, the frequency response of the light path between transmitter and receiver may be expressed as (after [1])

$$T^{(R)}(\omega) = \sum_{m=1}^{M} A_m^{(R)}(\omega) \tag{3}$$

In the following, we shortly describe all the modeled elements.

2.1. Light source

The initial mode group power vector $\mathbf{A}^{(\text{inp})}$ depends obviously on the light source type. In the following, results will be shown for two standard excitations [3]: overfilled launch (OFL) modeling LED source and restricted mode launch (RML) modeling vertical cavity surface emitting laser (VCSEL), but the method is not limited to them. Those excitations have been standardized to eliminate the dependence of measured frequency response on light source type or specimen [3]. Any kind of light launch can be easily introduced in the numerical model.

2.2. Fiber

The derivation of the matrix representation for the fiber, that takes mode mixing effects into account, is described in detail in [4]. Here, to simplify the formalism, we neglect mode mixing, as it usually has negligible influence in GI silica fibers [1]. The fiber matrix is then a diagonal $M \times M$ matrix with elements [1]

$$\tilde{F}_{m, m} = \exp(-\gamma_m L - j\omega\tau_m L) \tag{4}$$

where γ_m and τ_m are the mode group dependent attenuation and the group delay, respectively, j is the imaginary unit and L is the fiber's length.

2.3. Connector

Our approach to the connector modeling follows [1]. The connector transfer matrix can be found by finding the expansion coefficients of the input fiber modes in the basis of the output fiber modes.

2.4. Coupler/splitter

To obtain coupler matrices (one for each arm), the simplified wave equation for inhomogeneous coupler structure has to be solved repeatedly for all modes propagating in the couplers' medium [5]:

$$\left\{ i2kn_2 \frac{\partial}{\partial z} + \frac{\partial^2}{\partial x^2} + \frac{\partial^2}{\partial y^2} + k^2 \left[n_1^2(x, y, z) - n_2^2 \right] \right\} \varphi_{\mu, \nu}(x, y, z) = 0 \tag{5}$$

where k is the wave constant, n_2 is the refractive index of the cladding, $n_1(x, y, z)$ is the refractive index value in the mesh point and $\varphi_{\mu, \nu}(x, y, 0)$ is the field distribution of the fiber $LP_{\mu, \nu}$ mode. Hence, two spatial amplitude fields $\varphi_{\mu, \nu}^{(\text{out})}(x, y)$ at far ends of both arms of the coupler are obtained. In the next step they are decomposed into orthogonal set of modes by calculating following integrals

$$a_{\mu, \nu}^{\mu', \nu'} = \iint_S \mathrm{d}x\mathrm{d}y\, \varphi_{\mu', \nu'}^*(x, y)\varphi_{\mu, \nu}^{(\text{out})}(x, y) \tag{6}$$

Analogously to the connector case [1] the coupler power transfer matrix is obtained as follows

$$\tilde{S}_{m', m} = \frac{1}{2m} \sum_{\mu', \nu', \mu, \nu} \left| a_{\mu, \nu}^{\mu', \nu'} \right|^2 \delta(m' - \mu' - 2\nu' + 1)\, \delta(m - \mu - 2\nu + 1) \tag{7}$$

where m is the mode group number, δ is the Kronecker's symbol, $2m$ stands for the number of modes in the m-th mode group. The decomposing procedure has to be repeated for two arms independently. This approach allows modeling of any coupler structure provided that its mechanical layout is known.

3. Results and measurements

We have examined various MMF PON structures of tree architectures both numerically and experimentally. We have calculated and measured frequency responses of various optical paths within such networks. The most important conclusion is that these responses are different for different paths for otherwise symmetrical network. This implies that the 3 dB bandwidths of various paths are not equal and may differ by a few tens of percent. The reason behind this is that splitters perform mode filtering differently in each arm (in the numerical model, the matrices are different in each of the splitters arms). If one of the arms of a multimode coupler is excited, the higher order modes (propagate near the cladding and may have higher angles in the geometrical approximation) tend to couple into the second arm of the coupler, whereas the lower order modes (propagate in the core center and have smaller angles) tend to stay in the first arm. Thus, the transmission matrix of a coupler with a geometry we consider, is typically different in its different branches. This effect is most pronounced in a single splitter network, whereas it tends to be averaged in more complex architectures.

According to our knowledge, the most popular couplers used in PON networks are side couplers, and only those are considered in this paper. They consist of two multimode fibers that are gradually brought close together, so that their modal fields overlap and energy transfer from the input arm to the lateral arm is enabled, and then they are gradually separated (example structure in Fig. 1). The coupling region can be additionally fused and tapered, to improve coupling efficiency. However, the exact geometrical layout of the coupler remains manufacturer's secret. In our simulations, we consider the coupler structure presented in Fig. 1.
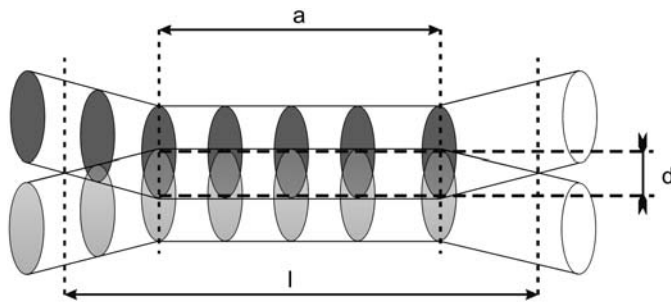

Fig. 1. Geometry of the considered coupler. Exact parameters given in the Table.

T a b l e. Geometrical parameters of couplers used in calculations.

Coupler No.	a [mm]	l [mm]	d [μm]
1	1.2	3.4	8
2	1.3	3.5	10
3	1.4	3.6	15

To show the effect of coupler filtering, we present results for a MMF (1 km long, 62.5 μm, NA = 0.275, graded index, with a profile flaw in the core center, and profile parameter selected to match the measurement data) which is connected to a 2×2 coupler either at its front or at its end. To get greater variety of results in calculations, we considered 3 realizations of coupler structure, of geometrical parameters given in the Table, that were numerically designed to give splitting ratio close to 50/50 at 850 nm wavelength. All possible to acquire frequency responses are plotted in Figs. 2 and 3 for OFL and RML, respectively. For comparison, results of measurements of analogous network incorporating 4 different commercial couplers from the same
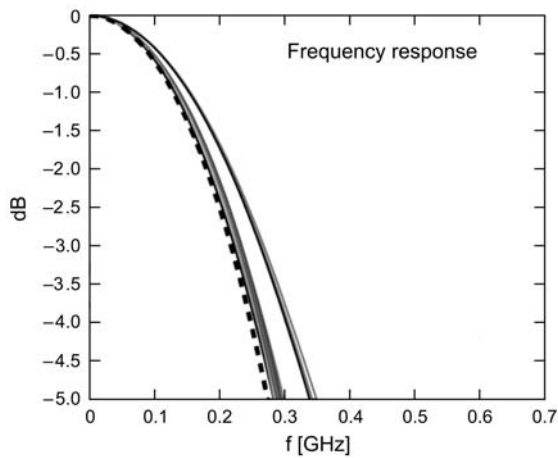

Fig. 2. Calculated frequency responses of a fiber interconnected with various couplers either on its input or output, in different arms. The dotted curve is the frequency response of the fiber itself. OFL.
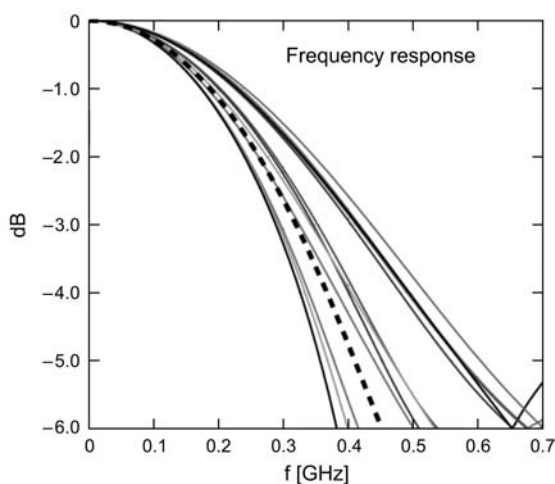

Fig. 3. Calculated frequency responses of a fiber interconnected with various couplers either on its input or output, in different arms. The dotted curve is the frequency response of the fiber itself. RML.
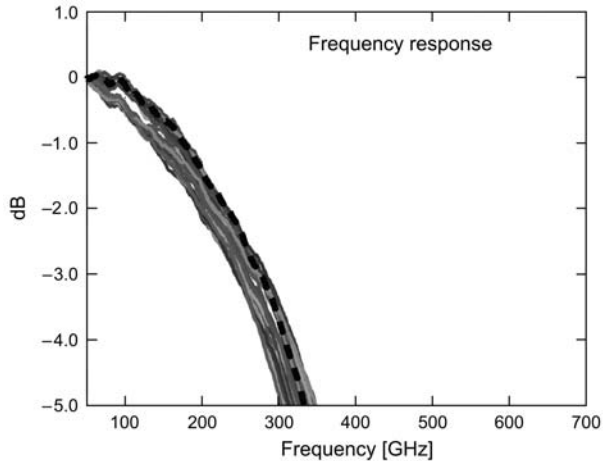
Fig. 4. Measured frequency responses of a fiber interconnected with various couplers either on its input or output, in different arms. The dotted curve is the frequency response of the fiber itself. OFL.
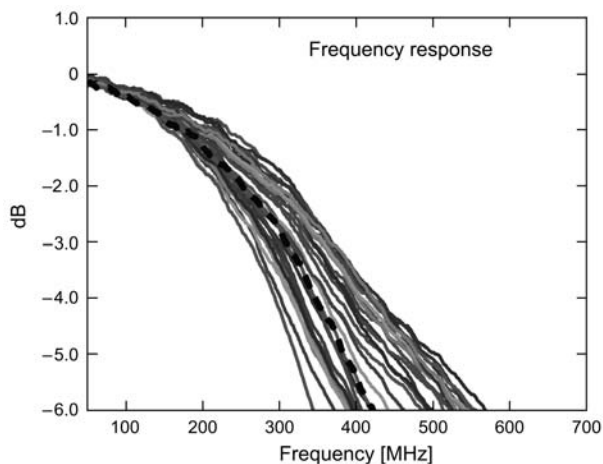

Fig. 5. Measured frequency responses of a fiber interconnected with various couplers either on its input or output, in different arms. The dotted curve is the frequency response of the fiber itself. RML.

production series are depicted in Figs. 4 and 5 [6]. As we can see, the bandwidth is different in different coupler branches, and the variations can be even as high as 30% for RML and 15% for OFL. The dotted curve in each figure is the frequency response of the examined fiber itself (without coupler/splitter). It may be treated as the first approximation of the bandwidth in the network, however, it may not be considered as the upper or the lower bound.

Unfortunately, direct comparison of measured and calculated results is not possible. The calculation of a real commercial coupler matrix was not possible as the physical layout of the commercial couplers was not available, and it is evident that different

coupler types have different mode filtering properties. However, the proposed method allows modeling of any coupler structure, provided that the physical layout of the coupler geometry is known.

4. Summary

We introduced an extension of MMF link model [1], that allows numerical calculation of frequency response in MMF PON networks. It was shown that otherwise identical paths in MMF PON have different bandwidths. This follows from filtering properties of MMF couplers/splitters. The differences in bandwidth between the nodes are the highest for RML, which unfortunately is a typical launch in contemporary MMF systems. It is shown that the splitter may improve or decrease the bandwidth of a fiber itself, and that the bandwidth of optical fiber of equivalent length is a first approximation of the network bandwidth.

References

[1] PEPELJUGOSKI P., GOLOWICH S.E., RITGER A.J., KOLESAR P., RISTESKI A., *Modeling and simulation of next generation multimode fiber links*, Journal of Lightwave Technology **21**(5), 2003, pp. 1242–1255.

[2] RADDATZ L., WHITE I.H., CUNNINGHAM D.G., NOWELL M.C., *An experimental and theoretical study of the offset launch technique for the enhancement of the bandwidth of multimode fiber links*, Journal of Lightwave Technology **16**(3), 1998, pp. 324–331.

[3] FOTP-204, *Measurement of bandwidth of multimode fiber*, 2000.

[4] STĘPNIAK G., SIUZDAK J., *An efficient method for calculation of the MM fiber frequency respose in the presence of mode coupling*, Optical and Quantum Electronics **38**(15), 2006, pp. 1195–1201.

[5] YEH C., BROWN W.P., SZEJN R., *Multimode inhomogeneous fiber couplers*, Applied Optics **18**(4), 1979, pp. 489–495.

[6] MAKSYMIUK L., STEPNIAK G., SIUZDAK J., *Measurements of multimode fiber PON bandwidth*, Proceedings of IEEE/LEOS AOE, October 2007, Shanghai, China, pp. 263–265.